

Published in final edited form as:

Neurotoxicology. 2014 December ; 0: 285–292. doi:10.1016/j.neuro.2014.03.007.

Vulnerability of Welders to Manganese Exposure – A Neuroimaging Study

Long Zaiyang^{*†}, Jiang Yue-Ming[‡], Li Xiang-Rong[§], Fadel William[¶], Xu Jun^{*†}, Yeh Chien-Lin^{*†}, Long Li-Ling[§], Luo Hai-Lan[‡], Harezlak Jaroslaw^{¶,||}, Murdoch James B^{||l}, Zheng Wei^{*}, and Dydak Ulrike^{*†}

^{*}School of Health Sciences, Purdue University, West Lafayette, IN, USA

[†]Department of Radiology and Imaging Sciences, Indiana University School of Medicine, Indianapolis, IN, USA

[‡]Department of Health Toxicology, Guangxi Medical University, Nanning, China

[§]Department of Radiology, the First Affiliated Hospital of Guangxi Medical University, Nanning, China

[¶]Department of Biostatistics, Richard M. Fairbanks School of Public Health, Indiana University, Indianapolis, IN

^{||}Department of Biostatistics, Indiana University School of Medicine, Indianapolis, IN, USA

^{||l}Toshiba Medical Research Institute USA, Mayfield Village, OH, USA

Abstract

Increased manganese (Mn) exposure is known to cause cognitive, psychiatric and motor deficits. Mn exposure occurs in different occupational settings, where the airborne Mn level and the size of respirable particulates may vary considerably. Recently the importance of the role of the cerebral cortex in Mn toxicity has been highlighted, especially in Mn-induced neuropsychological effects. In this study we used magnetic resonance imaging (MRI) to evaluate brain Mn accumulation using T1 signal intensity indices and to examine changes in brain iron content using T2* contrast, as well as magnetic resonance spectroscopy (MRS) to measure exposure-induced metabolite changes non-invasively in cortical and deep brain regions in Mn-exposed welders, Mn-exposed smelter workers and control factory workers with no measurable exposure to Mn. MRS data as well as T1 signal intensity indices and T2* values were acquired from the frontal cortex, posterior cingulate cortex, hippocampus, and thalamus. Smelters were exposed to higher air Mn levels and had a

© 2014 Elsevier B.V. All rights reserved.

Corresponding Author: Ulrike Dydak, School of Health Sciences, Purdue University, 550 Stadium Mall Drive, West Lafayette, IN 47907, Phone: (765) 494 0550, Fax : (765) 496 1377, udydak@purdue.edu. Co-corresponding Author: Jiang Yue-Ming, Department of Health Toxicology, Guangxi Medical University, Nanning, Guangxi Province, China, Phone: +86-771-5358539, ymjjiang@163.com.

Conflict of interest statement

The authors have no conflict of interest to declare.

Publisher's Disclaimer: This is a PDF file of an unedited manuscript that has been accepted for publication. As a service to our customers we are providing this early version of the manuscript. The manuscript will undergo copyediting, typesetting, and review of the resulting proof before it is published in its final citable form. Please note that during the production process errors may be discovered which could affect the content, and all legal disclaimers that apply to the journal pertain.

longer duration of exposure, which was reflected in higher Mn levels in erythrocytes and urine than in welders. Nonetheless, welders had more significant metabolic differences compared to controls than did the smelter workers, especially in the frontal cortex. T1 hyperintensities in the globus pallidus were observed in both Mn-exposed groups, but only welders showed significantly higher thalamic and hippocampal T1 hyperintensities, as well as significantly reduced T2* values in the frontal cortex. Our results indicate that (1) the cerebral cortex, in particular the frontal cortex, is clearly involved in Mn neurotoxic effects and (2) in spite of the lower air Mn levels and shorter duration of exposure, welders exhibit more extensive neuroimaging changes compared to controls than smelters, including measurable deposition of Mn in more brain areas. These results indicate that the type of exposure (particulate sizes, dust versus fume) and route of exposure play an important role in the extent of Mn-induced toxic effects on the brain.

Keywords

manganese neurotoxicity; magnetic resonance spectroscopy; magnetic resonance imaging; frontal cortex; welding; smelting

1. Introduction

As an essential trace element, manganese (Mn) is required for maintaining normal function in the human body. However, excessive exposure to Mn has been associated with Parkinson-like symptoms including cognitive, psychiatric and motor deficits, as first described by Couper (1837) and currently known as manganism (Pal et al., 1999; Aschner and Aschner, 2005; Josephs et al., 2005; Zheng et al., 2011). Moreover, occupational and environmental exposure to Mn is well documented to lead to significant neurotoxic effects, namely detrimental effects on neuropsychological functions, some of which persist or worsen after cessation of exposure (Mergler et al., 1994; Lucchini et al., 1999; Josephs et al., 2005; Josephs et al., 2005; Bowler et al., 2006; Greiffenstein and Lees-Haley, 2007; Menezes-Filho et al., 2009; Bowler et al., 2011; Roels et al., 2012; Meyer-Baron et al., 2013; Zoni and Lucchini, 2013). The fact that cognitive changes are mostly associated with cortical brain regions, particularly the frontal cortex (Barbas, 2000; Chudasama and Robbins, 2006; Carter et al., 2009), emphasizes the importance of including cortical brain regions as targets for neuroimaging studies of Mn exposure.

Mn exposure is known to occur in different occupational settings, such as mining, steel and alloy production, welding, smelting, and dry-cell battery manufacturing, for which the types (i.e., fumes, inhalable dust) and levels of exposure can vary widely. Mn is a transition metal possessing multiple oxidation states capable of forming a series of oxides, among which Mn_3O_4 and MnO_2 have been identified and measured in both welding and smelting aerosols (Jiang et al., 2007; Cowan et al., 2009; Keane et al., 2010). Nonetheless, the type of exposure in these two occupations is quite different.

Welding is a major occupational activity worldwide. In the US, more than 462,000 workers are involved in welding operations as full-time welders or as a part of their jobs (Bureau of Labor Statistics, 2009). Welding joins metals using different thermal procedures such as electric arc or gas flame welding. Concentrated fumes containing vaporized metals and

metal oxides are produced during the welding process. In these fumes, the diameter of individual particles can be less than 0.01 μm (Zimmer, 2002), and aggregation can result in particulates generally smaller than 1 μm in diameter (Sowards et al., 2010). More than 90% of the Mn-containing welding aerosol is composed of respirable particulates (particle size < 10 μm) that can penetrate deeply into the lung. These Mn particulates may deposit in the alveoli and be converted to chemical forms of Mn (e.g. Mn^{2+}) that are readily available for systemic absorption (Aschner et al., 2005). In an animal inhalation model, Mn from inhaled Mn-containing particulates has also been identified in the olfactory bulb, from whence it can be transported along the olfactory nerve further into the brain (Elder et al., 2006). However, the exact brain regions for Mn translocation and the resulting concentrations are still under debate (Dorman et al., 2002). More recently, Sen et al. used MR imaging to detect Mn in the olfactory bulb of asymptomatic welders (Sen et al., 2011).

Smelting, on the other hand, involves extraction of metals from their ores using heat and chemical agents. Aerosols generated during smelting processes contain both fumes and coarser dust particulates and are less well characterized than the welding fume aerosols. Penetration and deposition of the particulate matter in the respiratory tract is particle-size selective. Apart from respirable particulates, the aerosols from smelting operations may also contain a significant amount of biologically relevant non-respirable Mn particles (particle size 10 to 100 μm), which may enter into the gastrointestinal tract via the mucociliary escalator and lead to Mn absorption at a rate equivalent to that of oral Mn intake. For smelters, the non-respirable fraction is roughly 10% of the inhalable fraction of the aerosol (Ellingsen et al., 2003).

Magnetic resonance imaging (MRI) and spectroscopy (MRS) can be used to evaluate the accumulation of Mn in the brain and to determine Mn exposure-induced metabolite changes non-invasively. Paramagnetic Mn ions shorten proton relaxation times, yielding hyperintense signals in T1-weighted MR images of the brain. Signal intensity indices from T1-weighted images can be used as an indicator of Mn accumulation, which has been associated with gliosis and neurodegeneration (Newland, 1999; Pal et al., 1999). Increased signal intensity indices have been observed in the globus pallidus, caudate, putamen, and the olfactory bulb as a result of Mn exposure (Nelson et al., 1993; Kim et al., 1999; Josephs et al., 2005; Dorman et al., 2006A; Criswell et al., 2012). In addition, increased iron (Fe) concentration in the brain gives rise to local magnetic field inhomogeneities that increase proton spin dephasing and thus shorten the T2* relaxation time. The measurement of T2* values has therefore been used to evaluate tissue Fe concentration (Haacke et al., 2005). Brain Fe concentration is known to be elevated in the substantia nigra, globus pallidus and caudate of patients with Parkinson's disease (Dexter et al., 1987; Griffiths and Grossman, 1993; Batista-Nascimento et al., 2012; Rossi et al., 2014); however, it is much less studied in Mn-exposed workers. Several MRS studies have investigated Mn-induced neurochemical changes and some of the results seem to be inconsistent, such as decreased or no change of frontal N-acetyl aspartate (NAA) (Guilarte et al., 2006; Kim et al., 2007; Chang et al., 2009; Dydak et al., 2011; Long et al., 2014). In this study we present data on the effect of Mn exposure on metabolite levels, T1 signal hyperintensities and T2* values in two cortical and two deep brain regions for two different occupational settings with Mn exposure: welding and smelting.

2. Materials and Methods

2.1. Subjects

14 male Mn-exposed welders (age (Median (Quantile 1, Quantile 3)), 30.5 (29.0, 37.3) years), 9 male Mn-exposed smelters (age 40.0 (33.0, 43.0) years) from two factories (a Mn-Fe alloy factory and a construction machinery factory), and 23 age- and gender-matched controls who were manual workers with no history of Mn exposure (age 31.0 (26.5, 45.5) years), were recruited from Guangxi Province, China. All workers had no history of neurological or psychiatric disorders, and have worked a minimum of three years at their current job and work five 8-h days per week. Stationary air sampling was carried out similarly to that in a previous study (Jiang et al., 2007), using a Model BFC-35 pump equipped with a micro-porous filter (diameter of 40mm, pore size 0.8 μ m). Samples were collected for more than 10 working shifts at three locations within each work environment and then averaged to obtain a representative air Mn level for each group. No personal air sampling was performed. For the control group, airborne Mn values were below the limit of quantification of the flame atomic absorption spectrometric method (AAS) (Shimadzu Model AA-6800, Japan). Blood and urine samples were collected in the morning of the examination day (a weekend day) and processed using the same method as described previously (Jiang et al., 2007). Mn concentrations in erythrocytes and urine were determined using a model JY-70PII inductively coupled plasma-atomic emission spectrophotometer (ICP-AES, JY70P Type II, Jobin-Yvon Company, France). The detection limit for Mn using this method was 0.3 ng/ml.

The study protocol was reviewed and approved by the Human Subjects Institutional Review Board at both Purdue University, USA, and Guangxi Medical University, China. Written informed consent was obtained from each subject prior to participation in the study.

2.2. MR imaging and spectroscopy

MRI and MRS scans were performed on a 3T Philips Achieva whole-body clinical scanner (Philips Healthcare, Best, the Netherlands), equipped with an eight-channel head coil. Fast T2-weighted images were acquired for exact planning of the VOIs using a turbo spin-echo sequence (TR/TE=3000/80ms, flip angle=90°, bandwidth=204 Hz/pixel, 17 slices, slice thickness=4 mm, field of view=230 \times 184 mm², acquisition matrix: 400 \times 320, resolution=0.5 \times 0.5 \times 4 mm³, SENSE factor 2). Short echo time ¹H spectra (PRESS localization; TR/TE=1500/30ms; CHESS water suppression) were acquired in each subject from four volumes of interest (VOIs): frontal cortex (20 \times 20 \times 20 mm³), posterior cingulate cortex (PCC) (30 \times 35 \times 25mm³), right hippocampus (30 \times 10 \times 10 mm³), and a 30 \times 30 \times 25 mm³ voxel centered on the right thalamus, but also containing portions of the globus pallidus, putamen, and other basal ganglia structures. To keep the overall scan time per subject on the order of 1 hour, the two off-center VOIs were only measured in the right brain hemisphere, assuming symmetric deposition and toxic effects of Mn as previously reported (Aschner and Aschner, 2005; Dorman et al. 2006A; Kim et al., 1999). The positioning of the VOIs is shown in Figure 1 and each VOI is centered at the Montreal Neurological Institute (MNI) coordinate [0, 46, 0], [0 -60, 24], [-26 -20 -21], [-19, -14, -3], respectively. For all of the VOIs, a reference spectrum was acquired without water suppression. These reference spectra

were then used for phase and frequency correction of the corresponding water-suppressed spectra, and additionally as a concentration reference for water-scaled metabolite ratios. Shimming and other preparation phases were performed fully automatically, resulting in line widths of < 15 Hz for the unsuppressed water peak for all spectra.

MRS data processing and quantification were performed with LCModel (Provencher, 1993), fitting each spectrum as a weighted linear combination of *in vitro* basis spectra from individual metabolite solutions. This basis set included NAA, myo-inositol (mI), creatine (Cr), glutamate (Glu), glutamine (Gln), glycerophosphocholine (GPC), phosphocholine (PCh), N-acetylaspartylglutamate (NAAG), and a number of minor metabolites. Three metabolite sums were examined as well: total choline (Cho) = GPC + Ph, total NAA = NAA + NAAG, and Glx = Glu + Gln. LCModel also adds a series of macromolecule (MM) peaks in the fitting process, in particular MM20, the component centered at a chemical shift of 2.0 ppm. All metabolite concentrations were scaled with respect to the unsuppressed water signal. However, because no corrections for relaxation were applied, concentrations are expressed here in institutional units. LCModel also reports an estimated relative standard deviation (%SD) for each metabolite and MM peak. Only fitting results with %SD values < 20% were used for further statistical analysis.

High-resolution 3D T1-weighted fast-gradient echo images (TR/TE=9.7/4.6ms, flip angle=8°, bandwidth=142 Hz/pixel, 120 slices, slice thickness=1.25 mm, field of view=240×240×150 mm³, acquisition matrix: 240×240, resolution=1×1×1.25 mm³, SENSE factor 2) were used to calculate the regional signal intensity index, which was defined as the ratio of T1-weighted signal in a region of interest (ROI) within each of the four MRS VOIs to the same neck muscle reference ROI, sized 35 mm² in area. The positions of the ROIs are centered at the MNI coordinate [0, 57, 8], [0 -44, 38], [24 -15 -12], [6, -14, 11], [0, -102, -103], respectively (Fig. 2). In addition, a fifth ROI for image analysis, centered at the MNI coordinate [16, 5, 2], was placed in the globus pallidus, which can show extensive Mn deposition and thus T1 hyperintensity. The positions of the ROIs for calculating T1 signal intensity indices are shown in Fig. 2. T2* maps using a fast field echo sequence (TR/first_TE/delta_TE: 24.5/3.7/4.4, flip angle=20°, bandwidth=287 Hz/pixel, 80 slices, slice thickness: 1.5mm, field of view=240×180 mm², acquisition matrix: 160×120, resolution=1.5×1.5×1.5 mm³, SENSE=2) were also acquired and used for estimating T2* values in the four ROIs. T2* values were calculated by fitting the signal intensity as a function of echo time using an exponential decay model.

2.3. Statistics

All analyses were carried out in R-2.15.1 (R Core Development System: <http://www.r-project.org>). Due to the limited sample size and asymmetric data distributions, all analyses were performed using nonparametric methods. To assess whether any differences existed among the smelters, welders, and controls, we performed Kruskal-Wallis tests in place of the usual ANOVA models that are only appropriate for normally distributed data. Only when these tests indicated a significant difference were two-way comparisons among all three groups then performed using Wilcoxon rank-sum pairwise tests with the significance level set at alpha = 0.05. To control for multiple testing, we used a false discovery rate with

q-value = 0.20 as a cutoff, i.e. only results with a q-value = 0.20 are reported as significant. Using 0.20 as our cutoff, we acknowledge that on average 20% of the significant findings identified could potentially be false positives (Benjamini and Hochberg 1995).

3. Results

The smelter group had both significantly longer years of exposure and higher airborne Mn (as MnO₂) levels than the welders, as shown in Table 1. Moreover, smelters had significantly higher erythrocyte Mn than welders and controls, as well as higher urine Mn than both welders and controls. Welders had higher erythrocyte Mn and urine Mn than controls. Age did not differ significantly among the three groups.

Table 2 summarizes the T1 signal intensity indices, T2* values, and metabolite levels in the different brain regions for the three groups. Metabolite levels are expressed as ratios to the unsuppressed water signal as reference, with appropriate correction factors applied in LCModel to yield approximate concentrations. As noted above, q-values were less than 0.2 for all reported significant results. Figure 1 depicts the VOIs for the four brain regions chosen for metabolic evaluation and a representative spectrum for each region from a control subject. In the frontal cortex VOI, reduced Glu (p<0.01), reduced Cr (p<0.05) and increased MM20 (p<0.05) were measured in welders compared to controls, whereas smelters showed only reduced Glu compared to controls (p<0.05). In the thalamus VOI, decreased mI was found in both smelters and welders (both p<0.01) compared to controls. In the PCC VOI, Cho and mI were both reduced in welders (both p<0.05), while only mI was decreased in smelters (p<0.05) compared to controls. No significant differences were found in the hippocampus VOI.

Figure 3 contains representative T1-weighted axial brain images of a welder (A), a smelter (B) and a control subject (C), displaying an obvious hyperintensity of the globus pallidus in the Mn-exposed workers. Accordingly, the T1 signal intensity indices were significantly elevated in the globus pallidus for both welders (p<0.01) and smelters (p<0.05) compared to controls. However, in the other four VOIs, only welders showed significant changes: higher thalamic and hippocampal T1 signal intensity indices compared to controls (p<0.01 and p<0.0001, respectively). Welders also had a significantly higher hippocampal T1 signal intensity index than smelters (p<0.05). In addition, T2* values were significantly decreased in the frontal cortex of welders compared to controls (p<0.05), but not so for smelters. No significant changes in T2* were observed in the other VOI's for either group.

4. Discussion

Welding and smelting are two different occupations that both involve exposure to airborne Mn. The results of this study show clearly that if the risk for neurotoxic effects in a particular occupational group is to be evaluated, assessment of air Mn levels and duration of exposure are not sufficient. The higher air Mn values and longer duration of exposure of the smelter group compared to the welder group are reflected in higher erythrocyte and urine Mn levels in the smelters. However, despite the higher level and duration of exposure, fewer changes in metabolism were observed in the smelters (decreased Glu in the frontal cortex, and reduced mI in the thalamus and PCC compared to controls) than in the welders, and

none of the brain regions investigated other than the globus pallidus area showed Mn accumulation in the smelters. In the welder group, we found significant changes of three metabolic moieties (Glu, Cr and MM20) in the frontal cortex, one (mI) in the thalamus, and two (Cho and mI) in the PCC compared to controls. In addition, welders also had higher thalamic and hippocampal T1 signal indices and tended to show a high frontal T1 signal index, indicating higher Mn accumulation in these regions. Moreover, welders showed significantly decreased T2* values in the frontal cortex, the likely result of higher Fe content in this region. These neuroimaging results suggest that even with lower exposure levels, the welders were affected more.

Kim et al. (1999) reported that 73.5% of welders while only 10.3% of smelters showed increased T1 signal intensities in the globus pallidus. These results are generally in line with our findings, although the authors did not provide the percentage increases in signal. While it is not clear what causes the more widespread effects in welders, it seems plausible that they are related to differences in the type of exposure between the two groups of Mn-exposed workers. Welding aerosols have been well characterized in the literature, with a fraction of respirable particulates over 90%, and most of these being fine respirable particulates (<1 μ m) (Ellingsen et al., 2003). In contrast, not much is published about the aerosols that smelters are exposed to, except that they are a mixture of fumes (with small respirable particulates) and of dust (with larger respirable particulates as well as a small percentage of non-respirable particles). It is conceivable that the fine/ultrafine particles in the welding fumes penetrate and distribute more readily into the different brain areas (Dorman et al., 2002; Elder et al., 2006; Sen et al., 2011), especially via the olfactory route bypassing the blood-brain barrier, thereby causing the more widespread effects.

On the other hand, exposure to different metal mixtures should also be considered in both occupations. While the percentages of Fe and Mn are high in welding fumes, there are also other metals present such as aluminum (Al), copper and molybdenum (Li et al., 2004; Balkhyour and Goknil, 2010), depending on the components of the metal being welded, coatings, types of electrodes, etc. In our air sampling, the top 4 metals in welding fumes are Fe (45.5%), calcium (Ca, 34.3%), Al (6.7%), and Mn (5.6%), whereas those in smelting fumes are Ca (39.6%), Mn (25.5%), Fe (10.9%), and zinc (9.6%). In addition, even small amounts of other metals could potentially influence the overall neurotoxicity. Furthermore, welders may also be exposed to nonmetallic neurotoxic chemicals, such as carbon monoxide, phosgene and ozone, which may further influence the differences found in this study.

Due to the similarity of manganese to Parkinson's disease and a high degree of Mn accumulation in the basal ganglia (Nagatomo et al., 1999; Aschner et al., 2005), many mechanistic studies of Mn neurotoxicity have focused on the basal ganglia in the past, especially prior to 2000 (Bhargava 1987; Eriksson et al., 1992; Cano et al., 1996; Pal et al., 1999; Centonze et al., 2001; Fitsanakis et al., 2006). Yet the brain areas involved in these multiple reports of Mn-induced neuropsychological deficits, especially cognitive deficits, are to a large extent associated with cortical areas, in particular the frontal cortex (Barbas, 2000; Chudasama and Robbins, 2006; Carter et al., 2009). Both the results from this study as well as other studies in the past show that Mn-induced metabolic changes also occur in brain

regions other than the thalamus and basal ganglia, which were traditionally thought to be the main target of Mn toxicity. Recently the cerebral cortex, especially the frontal cortex, has been shown to be a major target as well (Guilarte et al., 2008; Guilarte, 2013; Verina et al., 2013). In animal studies, significantly increased amounts of Mn have been observed in the frontal cortex of rodents (Elder et al., 2006) and in non-human primates (Dorman et al., 2006B; Bock et al., 2008) after Mn inhalation exposure. Reduced frontal NAA/Cr was shown to correlate with cumulative Mn exposure in Mn-exposed smelters (Dydak et al., 2011). Decreased frontal mI/Cr was associated with verbal learning test scores and blood Mn levels in Mn-exposed welders (Chang et al., 2009). Moreover, decreased fractional anisotropy in frontal white matter was also reported in welders, indicating decreased frontal white matter microstructural integrity, which was also shown to be associated with subtle motor and cognitive deficits (Kim et al., 2011). Our decreased T2* values in the frontal cortex of welders indicate an increased concentration of Fe, which is known to be linked to increased oxidative stress, neuronal vulnerability and neurodegeneration (Zecca et al., 2004; Stankiewicz and Brass, 2009). Together these results point towards an intrinsic vulnerability of the frontal cortex to Mn-induced neurotoxicity, which is further supported by our observation that amongst the brain regions examined in this study, the largest number of metabolic changes among Mn-exposed workers was found in the frontal cortex. Furthermore, these metabolic and morphological changes in the frontal cortex corroborate the many recent results on cognitive deficits associated with occupational and environmental exposure to Mn.

Besides the frontal cortex, we also chose to study the thalamus, PCC and hippocampus. The hippocampus plays a vital role in memory, learning and spatial orientation, whereas the thalamus lies along cortico-thalamo-cortical pathways and is especially important for sensory and motor commands (Parkin, 1996; Akhondzadeh, 1999; Sherman, 2007). Both regions have been shown to have neurotoxic changes after Mn exposure (Finkelstein et al., 2007; Burton and Guilarte, 2009; Dydak et al., 2011). The PCC is one of the most metabolically active brain regions, and it has been linked to cognitive control, working memory, associative learning and emotional salience (Pearson et al., 2011; Leech et al., 2012). Metabolic changes in the frontal cortex, PCC and thalamus regions in this study may therefore be associated with Mn-induced neuropsychological and motor deficits.

In the last decade, several studies in humans and non-human primates investigated brain metabolite changes after exposure to Mn and showed diverging patterns of results. It needs to be pointed out that divergence in published MRS findings is not uncommon, unless standardized and rigorous MRS acquisition *and* analysis techniques are used, and described in the publications in sufficient detail for reproduction by an MRS expert (Bottomley, 1991). Kim *et al.* (2007) reported no significant changes in NAA/Cr, Cho/Cr and NAA/Cho ratios in the basal ganglia of welders and did not study other brain areas. Chang et al. (2009) investigated frontal grey matter and parietal white matter and only found decreased mI/Cr in the frontal cortex of welders. In our previous study of smelters, reduced NAA/Cr was only found in the frontal cortex, but not in the thalamus, putamen, or globus pallidus (Dydak et al., 2011). This frontal cortex finding was not reproduced in the current smelter population, possibly due to the small sample size or simply to the different type of exposure between the

two factory settings. Additionally, in our earlier study, a trend of reduced mI/Cr was observed but not reported in a larger thalamus-centered voxel (akin to the reduced thalamic mI levels found in the present study). In Mn-exposed monkeys, Guilarte *et al.* (2006) found decreased NAA/Cr in the parietal cortex and the frontal white matter but not in the striatum. Decreased NAA and Glu levels were reported in the hypothalamus of overnight food-suppressed rats after Mn dosing (Just *et al.*, 2011). The different results in these studies point out that a better understanding of the toxicodynamics of brain metabolites in Mn exposure requires consideration of the type and duration of exposure, the type and size of Mn particulates, the differences between humans and animal models, and characteristics of the subjects' working conditions, e.g. whether they wear respiratory protection or not.

Decreases of Glu, Cr and Cho as shown in the present study have not been reported previously in Mn-exposed workers, but have been demonstrated in other studies on Mn neurotoxicity and related diseases. In an MRS study on Mn-treated cultured cells, Glu was found to decrease in neurons and neuron-astrocyte co-cultures, and decreases in mI were also observed in the co-cultures (Zwingmann *et al.*, 2003). Glu plays an important role in the brain as the major excitatory neurotransmitter and a neuronal precursor for GABA (Erecinska *et al.*, 1990). Lower frontal Glu has been associated with cognitive deficits (Ernst *et al.*, 2010). Recently, decreased Cr in the putamen and the midbrain has been shown in idiopathic Parkinson's disease patients (O'Neill *et al.*, 2002; Hattingen *et al.*, 2009). Cr is the key metabolite involved in energy metabolism. A lower Cr level was also associated with mitochondrial degeneration in lead neurotoxicity (Meng *et al.*, 2003). mI/Cr and Cho/Cr ratios were reduced in patients with hepatic cirrhosis (Geissler *et al.*, 1997; Spahr *et al.*, 2000) who have elevated Mn in the blood and in the brain due to damaged liver function (Butterworth *et al.*, 1995; Choi *et al.*, 2005). In the PCC of welders, the decrease of Cho, an important component of the cell membrane, may possibly indicate decreased cell membrane turnover or myelin alteration in this region. In the current study, the reduced mI is in general agreement with Chang *et al.* (2009), although they observed a decrease in frontal grey matter but not in parietal white matter (the two areas they examined), whereas we found a decrease in the thalamus and PCC but could not confirm lower mI in the frontal cortex. The reduced levels of mI (a glial marker) in the thalamus and PCC may indicate damage to glial cells in these regions. Reduced mI has also been associated with decreased verbal memory capability and altered mental status (Ross *et al.*, 1994; Shawcross *et al.*, 2004; Chang *et al.*, 2009). Thus in this context it may reflect the neurotoxic effects of Mn exposure.

While parallels to other studies and potential explanations for the metabolite changes found in this study are given above, the emphasis of our results are not the single findings of a particular metabolic concentration change, but rather the clear difference in number and locations of differences found in the welder population compared to controls, versus the smelter population compared to controls. Indeed, we note that the individual metabolic findings of the current study could be confounded by several limitations. First, the number of the smelters and welders that could be recruited was rather small, leading to a large q-value in our multiple comparison statistics, i.e. 20% of the reported significant differences could be false positives. However, this caveat applies to all groups, and thus the difference between welders and smelters remains. Second, information about covariates, such as

education of the subjects or their possible Mn exposure outside of work, was unknown. Third, our stationary air sampling results represent average Mn levels for each group, which may underestimate the real exposure for each subject. Our results also indicate that measuring particle sizes in the air sampling is crucial for future studies that are to compare different occupational settings. Lastly, slight repositioning errors of the VOIs and ROIs may occur, although every effort has been made to ensure precise positioning among all subjects, such as using internal brain landmarks.

In spite of these limitations, our results allow for the conclusion that the frontal cortex shows a special vulnerability to Mn exposure, very much in line with early cognitive effects, and that more extensive Mn-induced neurotoxic changes can be found in welders than in smelters. Therefore the type of exposure and differences in occupational setting need to be considered when comparing different studies, and need to be carefully assessed in future studies evaluating the risk for neurotoxicity due to Mn exposure.

Supplementary Material

Refer to Web version on PubMed Central for supplementary material.

Acknowledgments

The authors thank Dr. Harry Roels for helpful suggestions, discussions and revisions of the manuscript.

Funding Source

This work was supported by National Institutes of Health/National Institute of Environmental Health Sciences R21 [grant number ES-017498], National Natural Science Foundation of China [grant numbers 81072320 and 30760210], the Major State Basic Research Development Program of China 973 Program [Grant Number 2012CB525001].

References

1. Akhondzadeh S. Hippocampal synaptic plasticity and cognition. *J Clin Pharm Ther.* 1999; 24(4): 241–8. [PubMed: 10475982]
2. Aschner JL, Aschner M. Nutritional aspects of manganese homeostasis. *Mol Aspects Med.* 2005; 26(4–5):353–62. [PubMed: 16099026]
3. Aschner M, Erikson KM, Dorman DC. Manganese dosimetry: species differences and implications for neurotoxicity. *Crit Rev Toxicol.* 2005; 35(1):1–32. [PubMed: 15742901]
4. Balkhyour MA, Goknil MK. Total fume and metal concentrations during welding in selected factories in Jeddah, Saudi Arabia. *Int J Environ Res Public Health.* 2010; 7(7):2978–87. [PubMed: 20717553]
5. Barbas H. Connections underlying the synthesis of cognition, memory, and emotion in primate prefrontal cortices. *Brain Res Bull.* 2000; 15:52(5):319–30. [PubMed: 10922509]
6. Batista-Nascimento L, Pimentel C, Menezes RA, Rodrigues-Pousada C. Iron and neurodegeneration: from cellular homeostasis to disease. *Oxid Med Cell Longev.* 2012:128647.10.1155/2012/128647 [PubMed: 22701145]
7. Benjamini Y, Hochberg Y. Controlling the False Discovery Rate: A Practical and Powerful Approach to Multiple Testing. *J R Statist Soc, B.* 1995; 57(1):289–300.
8. Bhargava HN. Effect of repeated administration of manganese on the striatal cholinergic and dopaminergic receptors in the rat. *Toxicol Lett.* 1987; 37(2):135–41. [PubMed: 3603588]

9. Bock NA, Paiva FF, Nascimento GC, Newman JD, Silva AC. Cerebrospinal fluid to brain transport of manganese in a non-human primate revealed by MRI. *Brain Res.* 2008; 1198:160–70. [PubMed: 18243167]
10. Bowler RM, Gysens S, Diamond E, Nakagawa S, Drezgic M, Roels HA. Manganese exposure: neuropsychological and neurological symptoms and effects in welders. *Neurotoxicology.* 2006; 27:315–26. [PubMed: 16343629]
11. Bowler RM, Gocheva V, Harris M, Ngo L, Abdelouahab N, Wilkinson J, et al. Prospective study on neurotoxic effects in manganese-exposed bridge construction welders. *Neurotoxicology.* 2011; 32(5):596–605. [PubMed: 21762725]
12. Bottomley PA. The trouble with spectroscopy papers. *Radiology.* 1991; 181(2):344–50. [PubMed: 1924769]
13. Bureau of Labor Statistics. Welding, soldering and brazing workers. United States Department of Labor. 2009
14. Burton NC, Guilarte TR. Manganese neurotoxicity: lessons learned from longitudinal studies in nonhuman primates. *Environ Health Perspect.* 2009; 117(3):325–32. [PubMed: 19337503]
15. Butterworth RF, Spahr L, Fontaine S, Layrargues GP. Manganese toxicity, dopaminergic dysfunction and hepatic encephalopathy. *Metab Brain Dis.* 1995; 10(4):259–67. [PubMed: 8847990]
16. Cano G, Suarez-Roca H, Bonilla E. Manganese poisoning reduces strychnine-insensitive glycine binding sites in the globus pallidus of the mouse brain. *Invest Clin.* 1996; 37:209–19. [PubMed: 8968129]
17. Carter, R.; Aldridge, S.; Page, M.; Parker, S. *The human brain book - an illustrated guide to its structure, function, and disorders.* New York: Dorling Kindersley Publishing; 2009. 1st American ed
18. Centonze D, Gubellini P, Bernardi G, Calabresi P. Impaired excitatory transmission in the striatum of rats chronically intoxicated with manganese. *Exp Neurol.* 2001; 172:469–76. [PubMed: 11716571]
19. Chang Y, Woo ST, Lee JJ, Song HJ, Lee HJ, Yoo DS, et al. Neurochemical changes in welders revealed by proton magnetic resonance spectroscopy. *Neurotoxicology.* 2009; 30(6):950–7. [PubMed: 19631686]
20. Choi Y, Park JK, Park NH, Shin JW, Yoo CI, Lee CR, et al. Whole blood and red blood cell manganese reflected signal intensities of T1-weighted magnetic resonance images better than plasma manganese in liver cirrhotics. *J Occup Health.* 2005; 47(1):68–73. [PubMed: 15703454]
21. Chudasama Y, Robbins TW. Functions of frontostriatal systems in cognition: comparative neuropsychopharmacological studies in rats, monkeys and humans. *Biol Psychol.* 2006; 73(1):19–38. [PubMed: 16546312]
22. Couper J. On the effects of black oxide of manganese when inhaled in the lungs. *Br Ann Med Pharmacol.* 1837; 1:41–2.
23. Cowan DM, Fan Q, Zou Y, Shi X, Chen J, Aschner M, et al. Manganese exposure among smelting workers: blood manganese-iron ratio as a novel tool for manganese exposure assessment. *Biomarkers.* 2009; 14(1):3–16. [PubMed: 19283519]
24. Criswell SR, Perlmutter JS, Huang JL, Golchin N, Flores HP, Hobson A, et al. Basal ganglia intensity indices and diffusion weighted imaging in manganese-exposed welders. *Occup Environ Med.* 2012; 69:437–43. [PubMed: 22447645]
25. Dexter DT, Wells FR, Agid F, Agid Y, Lee AJ, Jenner P, et al. Increased nigral iron content in postmortem parkinsonian brain [letter]. *Lancet.* 1987; 2:1219–20. [PubMed: 2890848]
26. Dorman DC, Breneman KA, McElveen AM, Lynch SE, Roberts KC, Wong BA. Olfactory transport: a direct route of delivery of inhaled manganese phosphate to the rat brain. *J Toxicol Environ Health A.* 2002; 65(20):1493–511. [PubMed: 12396865]
27. Dorman DC, Struve MF, Wong BA, Dye JA, Robertson ID. Correlation of brain magnetic resonance imaging changes with pallidal manganese concentrations in rhesus monkeys following subchronic manganese inhalation. *Toxicol Sci.* 2006A; 92(1):219–27. [PubMed: 16638924]

28. Dorman DC, Struve MF, Marshall MW, Parkinson CU, James RA, Wong BA. Tissue manganese concentrations in young male rhesus monkeys following subchronic manganese sulfate inhalation. *Toxicol Sci.* 2006B; 92(1):201–10. [PubMed: 16624849]
29. Dydak U, Jiang YM, Long LL, Zhu H, Chen J, Li WM, et al. In vivo measurement of brain GABA concentrations by magnetic resonance spectroscopy in smelters occupationally exposed to manganese. *Environ Health Perspect.* 2011; 119(2):219–24. [PubMed: 20876035]
30. Elder A, Gelein R, Silva V, Feikert T, Opanashuk L, Carter J, et al. Translocation of inhaled ultrafine manganese oxide particles to the central nervous system. *Environ Health Perspect.* 2006; 114(8):1172–78. [PubMed: 16882521]
31. Ellingsen DG, Hetland SM, Thomassen Y. Manganese air exposure assessment and biological monitoring in the manganese alloy production industry. *J Environ Monit.* 2003; 5(1):84–90. [PubMed: 12619760]
32. Erecinska M, Silver IA. Metabolism and role of glutamate in mammalian brain. *Prog Neurobiol.* 1990; 35:245–96. [PubMed: 1980745]
33. Eriksson H, Gillberg PG, Aquilonius SM, Hedstrom KG, Heilbronn E. Receptor alterations in manganese intoxicated monkeys. *Arch Toxicol.* 1992; 66(5):359–64. [PubMed: 1319135]
34. Ernest T, Jiang CS, Nakama H, Buchthal S, Chang L. Lower brain glutamate is associated with cognitive deficits in HIV patients: a new mechanism for HIV-associated neurocognitive disorder. *J Magn Reson Imaging.* 2010; 32(5):1045–53. [PubMed: 21031507]
35. Finkelstein Y, Milatovic D, Aschner M. Modulation of cholinergic systems by manganese. *Neurotoxicology.* 2007; 28(5):1003–14. [PubMed: 17920128]
36. Fitsanakis VA, Au C, Erikson KM, Aschner M. The effects of manganese on glutamate, dopamine and gamma-aminobutyric acid regulation. *Neurochem Int.* 2006; 48(6–7):426–33. [PubMed: 16513220]
37. Geissler A, Lock G, Frund R, Held P, Hollerbach S, Andus T, et al. Cerebral abnormalities in patients with cirrhosis detected by proton magnetic resonance spectroscopy and magnetic resonance imaging. *Hepatology.* 1997; 25(1):48–54. [PubMed: 8985263]
38. Greiffenstein MF, Lees-Haley PR. Neuropsychological correlates of manganese exposure: a meta-analysis. *J Clin Exp Neuropsychol.* 2007; 29(2):113–26. [PubMed: 17365247]
39. Griffiths PD, Crossman AR. Distribution of iron in the basal ganglia and neocortex in postmortem tissue in Parkinson's disease and Alzheimer's disease. *Dementia.* 1993; 4:61–5. [PubMed: 8358514]
40. Guilarte TR. Manganese neurotoxicity: new perspectives from behavioral, neuroimaging, and neuropathological studies in humans and non-human primates. *Front Aging Neurosci.* 2013; 5:23.10.3389/fnagi.2013.00023 [PubMed: 23805100]
41. Guilarte TR, Burton NC, Verina T, Prabhu VV, Becker KG, Syversen T, et al. Increased APLP1 expression and neurodegeneration in the frontal cortex of manganese-exposed non-human primates. *J Neurochem.* 2008; 105(5):1948–59. [PubMed: 18284614]
42. Guilarte TR, McGlothlan JL, Degaonkar M, Chen MK, Barker PB, Syversen T, et al. Evidence for cortical dysfunction and widespread manganese accumulation in the nonhuman primate brain following chronic manganese exposure: a 1H-MRS and MRI study. *Toxicol Sci.* 2006; 94(2):351–8. [PubMed: 16968886]
43. Haacke EM, Cheng NY, House MJ, Liu Q, Neelavalli J, Ogg RJ, et al. Imaging iron stores in the brain using magnetic resonance imaging. *Magn Reson Imaging.* 2005; 23(1):1–25. [PubMed: 15733784]
44. Hattingen E, Magerkurth J, Pilatus U, Mozer A, Seifried C, Steinmetz H, et al. Phosphorus and proton magnetic resonance spectroscopy demonstrates mitochondrial dysfunction in early and advanced Parkinson's disease. *Brain.* 2009; 132:3285–97. [PubMed: 19952056]
45. Jiang Y, Zheng W, Long L, Zhao W, Li X, Mo X, et al. Brain magnetic resonance imaging and manganese concentrations in red blood cells of smelting workers: search for biomarkers of manganese exposure. *Neurotoxicology.* 2007; 28(1):126–35. [PubMed: 16978697]
46. Josephs KA, Ahlskog JE, Klos KJ, Kumar N, Fealey RD, Trenerry MR, et al. Neurologic manifestations in welders with pallidal MRI T1 hyperintensity. *Neurology.* 2005; 64(12):2033–39. [PubMed: 15888601]

47. Just N, Cudalbu C, Lei H, Gruetter R. Effect of manganese chloride on the neurochemical profile of the rat hypothalamus. *J Cereb Blood Flow Metab.* 2011; 31(12):2324–33. [PubMed: 21712832]
48. Keane M, Stone S, Chen B. Welding fumes from stainless steel gas metal arc processes contain multiple manganese chemical species. *J Environ Monit.* 2010; 12(5):1133–40. [PubMed: 21491680]
49. Kim EA, Cheong HK, Choi DS, Sakong J, Ryoo JW, Park I, et al. Effect of occupational manganese exposure on the central nervous system of welders: 1H magnetic resonance spectroscopy and MRI findings. *Neurotoxicology.* 2007; 28(2):276–83. [PubMed: 16824604]
50. Kim Y, Kim KS, Yang JS, Park IJ, Kim E, Jin Y, et al. Increase in signal intensities on T1-weighted magnetic resonance images in asymptomatic manganese-exposed workers. *Neurotoxicology.* 1999; 2:901–7. [PubMed: 10693971]
51. Kim Y, Jeong KS, Song HJ, Lee JJ, Seo JH, Kim GC, et al. Altered white matter microstructural integrity revealed by voxel-wise analysis of diffusion tensor imaging in welders with manganese exposure. *Neurotoxicology.* 2011; 32(1):100–9. [PubMed: 21111757]
52. Leech R, Braga R, Sharp DJ. Echoes of the brain within the posterior cingulate cortex. *J Neurosci.* 2012; 32(1):215–22. [PubMed: 22219283]
53. Li GJ, Zhang LL, Lu L, Wu P, Zheng W. Occupational exposure to welding fume among welders: alterations of manganese, iron, zinc, copper, and lead in body fluids and the oxidative stress status. *J Occup Environ Med.* 2004; 46(3):241–8. [PubMed: 15091287]
54. Long Z, Li XR, Xu J, Edden RA, Qin WP, Long LL, Murdoch JB, Zheng W, Jiang YM, Dydak U. Thalamic GABA predicts fine motor performance in manganese-exposed smelter workers. *PLoS One.* 2014; 9(2):e88220. [PubMed: 24505436]
55. Lucchini R, Apostoli P, Perrone C, Placidi D, Albini E, Migliorati P, et al. Long-term exposure to “low levels” of manganese oxides and neurofunctional changes in ferroalloy workers. *Neurotoxicology.* 1999; 20:287–98. [PubMed: 10385891]
56. Menezes-Filho JA, Bouchard M, de Sarcinelli PN, Moreira JC. Manganese exposure and the neuropsychological effects on children and adolescents: a review. *Rev Panam Salud Publica.* 2009; 26(6):541–8. [PubMed: 20107709]
57. Meng XM, Ruan DY, Kang LD, Zhu DM, She JQ, Luo L, et al. Age-related morphological impairments in the rat hippocampus following developmental lead exposure: an MRI, LM and EM study. *Environ Toxicol Phar.* 2003; 13(3):187–97.
58. Mergler D, Huel G, Bowler R, Iregren A, Belanger S, Baldwin M, et al. Nervous system dysfunction among workers with long-term exposure to manganese. *Environ Res.* 1994; 64:151–80. [PubMed: 8306949]
59. Meyer-Baron M, Schaper M, Knapp G, Lucchini R, Zoni S, Bast-Pettersen R, et al. The neurobehavioral impact of manganese: results and challenges obtained by a meta-analysis of individual participant data. *Neurotoxicology.* 2013; 36:1–9. [PubMed: 23419685]
60. Nagatomo S, Umehara F, Hanada K, Nobuhara Y, Takenaga S, Arimura K, et al. Manganese intoxication during total parental nutrition: report of two cases and review of the literature. *J Neurol Sci.* 1999; 162(1):102–5. [PubMed: 10064179]
61. Nelson K, Golnick J, Korn T, Angle C. Manganese encephalopathy: utility of early magnetic resonance imaging. *Br J Ind Med.* 1993; 50:510–13. [PubMed: 8329316]
62. Newland MC. Animal models of manganese’s neurotoxicity. *Neurotoxicology.* 1999; 20:415–32. [PubMed: 10385901]
63. O’Neill J, Schuff N, Marks WJ Jr, Feiwell R, Aminoff MJ, Weiner MW. Quantitative 1H magnetic resonance spectroscopy and MRI of Parkinson’s disease. *Mov Disord.* 2002; 17(5):917–27. [PubMed: 12360540]
64. Pal PK, Samii A, Calne DB. Manganese neurotoxicity: a review of clinical features, imaging and pathology. *Neurotoxicology.* 1999; 20:227–38.
65. Parkin AJ. Human memory: the hippocampus is the key. *Curr Biol.* 1996; 6(12):1583–5. [PubMed: 8994819]
66. Pearson JM, Heilbronner SR, Barack DL, Hayden BY, Platt ML. Posterior cingulate cortex: adaptive behavior to a changing world. *Trends Cogn Sci.* 2011; 15(4):143–51. [PubMed: 21420893]

67. Provencher SW. Estimation of metabolite concentrations from localized in vivo proton NMR spectra. *Magn Reson Med*. 1993; 30(6):672–9. [PubMed: 8139448]
68. Roels HA, Bowler RM, Kim Y, Claus Henn B, Mergler D, Hoet P, et al. Manganese exposure and cognitive deficits: A growing concern for manganese neurotoxicity. *Neurotoxicology*. 2012; 33(4): 872–80. [PubMed: 22498092]
69. Ross BD, Jacobson S, Villamil F, Korula J, Kreis R, Ernst T, et al. Subclinical hepatic encephalopathy: proton MR spectroscopic abnormalities. *Radiology*. 1994; 193(2):457–63. [PubMed: 7972763]
70. Rossi ME, Ruottinen H, Saunamaki T, Elovaara I, Dastidar P. Imaging brain iron and diffusion patterns: a follow-up study of Parkinson's disease in the initial stages. *Acad Radiol*. 2014; 21(1): 64–71. [PubMed: 24331266]
71. Sen S, Flynn MR, Du G, Troster AI, An H, Huang X. Manganese accumulation in the olfactory bulbs and other brain regions of “asymptomatic” welders. *Toxicol Sci*. 2011; 121(1):160–7. [PubMed: 21307282]
72. Shawcross DL, Balata S, Olde Damink SW, Hayes PC, Wardlaw J, Marshall I, et al. Low myo-inositol and high glutamine levels in brain are associated with neuropsychological deterioration after induced hyperammonemia. *Am J Physiol Gastrointest Liver Physiol*. 2004; 287(3):G503–9. [PubMed: 15130875]
73. Sherman SM. The thalamus is more than just a relay. *Curr Opin Neurobiol*. 2007; 17(4):417–22. [PubMed: 17707635]
74. Sowards JW, Ramirez AJ, Dickinson DW, Lippold JC. Characterization of Welding Fume from SMAW Electrodes - Part II. *Weld J*. 2010; 89(4):82s–90s.
75. Stankiewicz JM, Brass SD. Role of iron in neurotoxicity: a cause for concern in the elderly? *Curr Opin Nutr Metab Care*. 2009; 12(1):22–9.
76. Spahr L, Vingerhoets F, Lazeyras F, Delavelle J, DuPasquier R, Giostra E, et al. Magnetic resonance imaging and proton spectroscopic alterations correlate with parkinsonian signs in patients with cirrhosis. *Gastroenterology*. 2000; 119(3):774–81. [PubMed: 10982772]
77. Verina T, Schneider JS, Guilarte TR. Manganese induces α -synuclein aggregation in the frontal cortex of non-human primates. *Toxicol Lett*. 2013; 217:177–83. [PubMed: 23262390]
78. Zecca L, Youdim MB, Riederer P, Connor JR, Crichton RR. Iron, brain ageing and neurodegenerative disorders. *Nat Rev Neurosci*. 2004; 5(11):863–73. [PubMed: 15496864]
79. Zheng W, Fu SX, Dydak U, Cowan DM. Biomarkers of manganese intoxication. *Neurotoxicology*. 2011; 32(1):1–8. [PubMed: 20946915]
80. Zimmer AT. The influence of metallurgy on the formation of welding aerosols. *J Environ Monit*. 2002; 4(5):628–32. [PubMed: 12400906]
81. Zoni S, Lucchini RG. Manganese exposure: cognitive, motor and behavioral effects on children: a review of recent findings. *Curr Opin Pediatr*. 2013; 25(2):255–60. [PubMed: 23486422]
82. Zwingmann C, Leibfritz D, Hazell AS. Energy metabolism in astrocytes and neurons treated with manganese: relation among cell-specific energy failure, glucose metabolism, and intercellular trafficking using multinuclear NMR-spectroscopic analysis. *J Cereb Blood Flow Metab*. 2003; 23(6):756–71. [PubMed: 12796724]

- In vivo brain metabolism and Mn deposition were explored in Mn-exposed workers
- Two occupational settings were compared: smelting and welding
- The frontal cortex shows the most pronounced metabolic changes
- The results suggest that welders are more susceptible to Mn-induced neurotoxicity

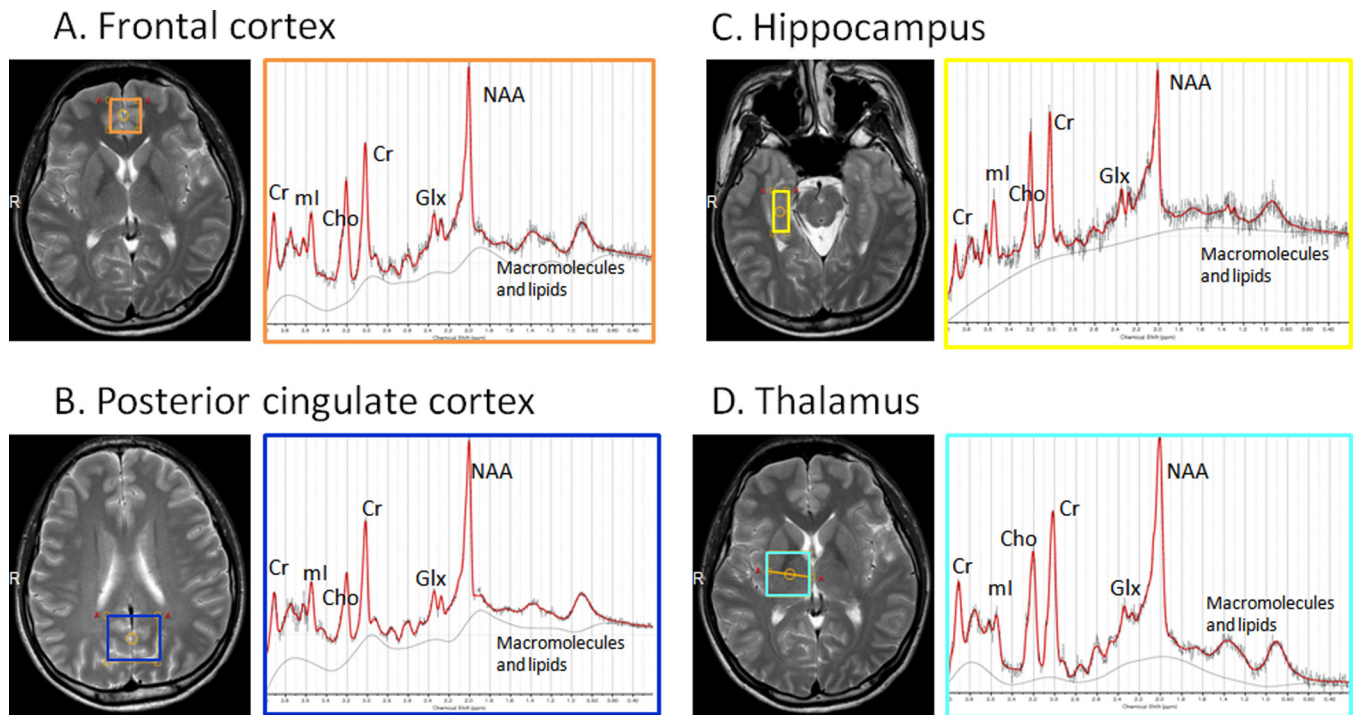


Figure 1. Volumes of interest (VOIs) for four brain regions and representative short-TE spectra with LCModel fitting for each region: A, frontal cortex; B, posterior cingulate cortex (PCC); C, hippocampus; D, thalamus.

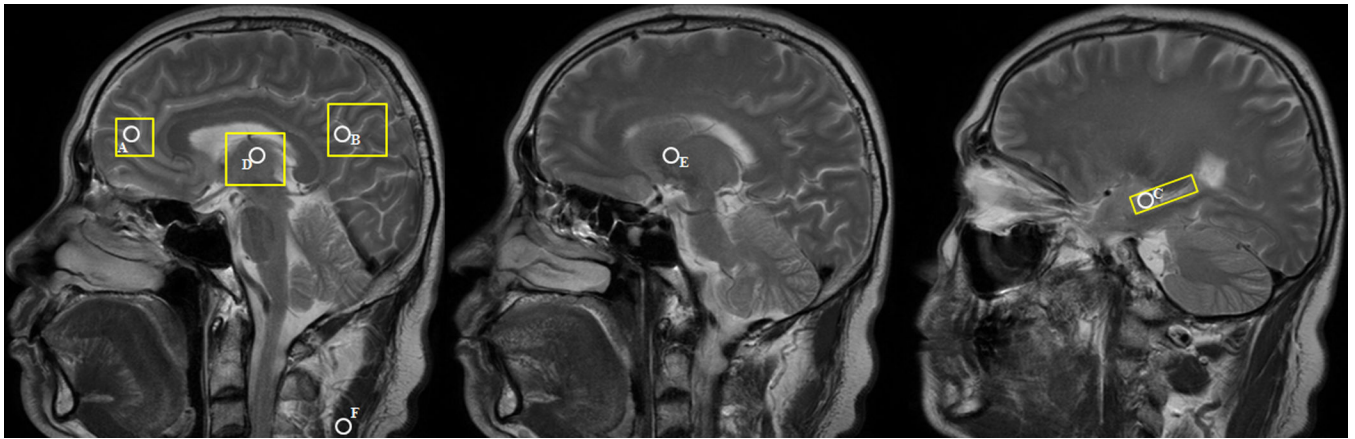


Figure 2.

Regions of interest (ROIs) for five brain regions: A, frontal cortex; B, posterior cingulate cortex (PCC); C, hippocampus; D, thalamus; E, globus pallidus; and F, a neck muscle reference region, for calculating T1 signal intensity indices and T2* values. Corresponding spectroscopy VOI's for A–D are highlighted in yellow.

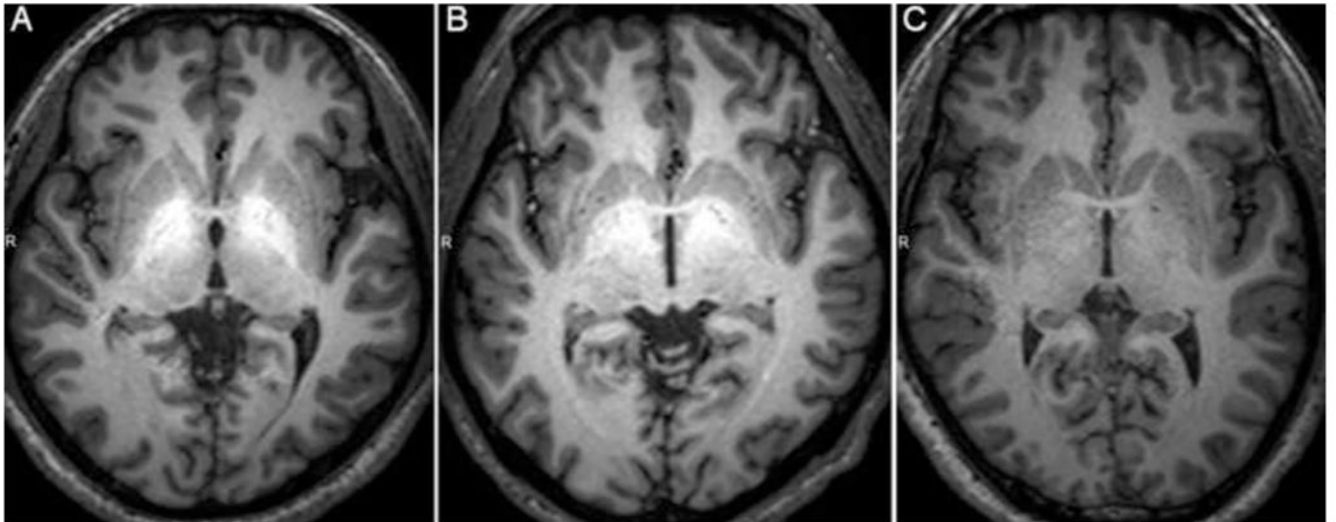


Figure 3. Representative axial T1-weighted MRI brain images of a welder (A), a smelter worker (B), and a control worker (C), displaying the hyperintense signal associated with brain manganese deposition, especially in the globus pallidus, in both Mn-exposed groups.

Table 1

Exposure information of Mn-exposed welders, smelters and controls (Median (Quartile 1, Quartile 3)).

	Welders	Smelters	Controls
Airborne MnO ₂ [mg/m ³]	0.03(0.02, 0.08) [#]	0.29(0.23, 0.39)	N
Years of exposure	8.0(5.0, 12.0) ^{##}	18.0(14.0, 25.0)	N/A
Erythrocyte Mn [mg/L]	0.9(0.8, 1.0) ^{*#}	1.3(1.2, 1.5) ^{**}	0.6(0.5, 0.7)
Urine Mn [μg/L]	20.0(15.0, 28.0) ^{**#}	37.5(29.6, 40.3) ^{**}	8.9(6.7, 10.8)

N: below the limit of quantification of the flame atomic absorption spectrometric method;

[#] p<0.05,^{##} p<0.01, for comparison between welders and smelters;^{*} p<0.05,^{**} p<0.01, for comparison between each Mn-exposed group and controls, respectively.

Table 2

Metabolite levels (scaled to brain water content, reported in institutional units), T1 signal intensity indices and T2* values (Median (Quartile 1, Quartile 3)) in four brain regions for smelters and welders compared to controls. In addition, T1 signal intensity indices for the globus pallidus are also included. Group comparisons were performed using Kruskal-Wallis tests followed by Wilcoxon pairwise tests (significant changes are highlighted in bold font). A false discovery rate control was used to correct for multiple comparisons and the results with $q < 0.20$ are reported.

Frontal Cortex			
	Controls	Welders	Smelters
N-acetyl-aspartate(NAA)	6.8(6.5, 7.1)	6.4(6.1, 6.7)	6.6(6.4, 6.9)
NAA+N-acetylaspartylglutamate(NAAG)	7.2(6.8, 7.5)	7.0(6.7, 7.3)	6.9(6.8, 7.1)
myo-inositol(ml)	5.9(5.4, 6.4)	6.1(5.6, 6.4)	5.8(5.0, 6.3)
creatine(Cr)	6.3(6.0, 6.6)	5.9(5.7, 6.1)*	6.3(5.8, 6.6)
glutamate(Glu)	8.4(7.8, 8.8)	7.8(7.1, 8.1)**	7.6(7.5, 8.2)*
Glu+Gln(Glx)	12.2(9.8, 12.8)	9.8(9.2, 11.7)	11.5(10.1, 12.2)
total choline(Cho)	1.8(1.7, 1.9)	1.7(1.6, 1.9)	1.9(1.8, 2.0)
MM09	7.5(6.8, 8.7)	8.3(7.9, 9.0)	7.9(7.2, 8.3)
MM20	12.6(11.2, 14.5)	13.9(13.3, 16.1)*	13.3(11.8, 14.6)
T1 Signal Intensity Index	1.3(1.2, 1.4)	1.4(1.3, 1.5)	1.3(1.1, 1.4)
T2* (ms)	62.5(58.1, 65.3)	57.4(55.5, 59.2)*	60.8(57.2, 66.0)
Thalamus			
	Controls	Welders	Smelters
N-acetyl-aspartate(NAA)	6.8(6.4, 7.0)	6.8(6.5, 7.0)	6.6(6.4, 6.9)
NAA+N-acetylaspartylglutamate(NAAG)	7.8(7.4, 8.1)	7.4(7.2, 7.5)	7.3(7.0, 7.8)
myo-inositol(ml)	4.5(4.1, 4.8)	3.9(3.6, 4.3)**	3.4(3.3, 3.9)**
creatine(Cr)	6.2(5.9, 6.4)	5.9(5.8, 6.2)	6.2(6.0, 6.4)
glutamate(Glu)	5.7(5.0, 6.5)	5.4(4.8, 6.0)	5.2(5.1, 5.5)
Glu+Gln(Glx)	8.3(7.2, 9.4)	7.2(6.4, 8.3)	7.3(7.2, 7.8)
total choline(Cho)	1.8(1.7, 2.0)	1.8(1.6, 1.9)	1.8(1.7, 2.0)
MM09	5.5(5.1, 6.1)	5.7(5.1, 6.0)	6.9(5.7, 6.2)
MM20	10.4(9.4, 10.9)	10.6(9.9, 11.8)	10.6(10.1, 11.6)
T1 Signal Intensity Index	1.4(1.1, 1.8)	1.8(1.7, 2.0)**	1.8(1.4, 2.0)
T2* (ms)	45.3(43.6, 49.7)	44.6(43.1, 49.4)	46.3(42.9, 50.8)
Posterior Cingulate Cortex			
	Controls	Welders	Smelters
N-acetyl-aspartate(NAA)	7.6(7.1, 8.0)	7.5(7.3, 8.0)	7.2(7.0, 7.8)
NAA+N-acetylaspartylglutamate(NAAG)	7.9(7.6, 8.1)	7.8(7.3, 8.0)	7.4(7.2, 7.8)
myo-inositol(ml)	5.2(5.1, 5.6)	4.9(4.6, 5.1)*	4.8(4.7, 5.1)*
creatine(Cr)	5.7(5.3, 6.1)	5.8(5.4, 6.0)	5.8(5.7, 6.2)
glutamate(Glu)	5.5(5.2, 6.0)	5.4(5.2, 6.0)	5.5(5.0, 5.7)

Posterior Cingulate Cortex			
Glu+Gln(Glx)	6.3(5.6, 7.1)	6.5(6.1, 6.8)	6.9(6.3, 7.3)
total choline(Cho)	1.1(1.0, 1.1)	1.0(0.9, 1.1)*	1.0(1.0, 1.0)
MM09	7.1(6.6, 8.4)	8.1(7.5, 8.7)	7.6(7.3, 8.4)
MM20	12.6(10.8, 13.6)	13.4(12.4, 14.2)	12.9(12.1, 13.8)
T1 Signal Intensity Index	1.6(1.4, 1.7)	1.5(1.4, 1.8)	1.2(1.1, 1.3)
T2* (ms)	54.5(48.3, 60.3)	56.0(53.4, 58.4)	56.8(55.6, 59.3)

Hippocampus			
	Controls	Welders	Smelters
N-acetyl-aspartate(NAA)	6.3(5.8, 6.7)	6.1(5.8, 6.4)	5.9(5.5, 6.4)
NAA+N-acetylaspartylglutamate(NAAG)	6.9(6.6, 7.3)	6.9(6.5, 7.3)	7.0(6.8, 7.5)
myo-inositol(ml)	6.7(6.4, 8.0)	6.4(5.8, 7.2)	6.9(6.0, 7.2)
creatine(Cr)	6.2(6.0, 6.6)	5.9(5.8, 6.4)	6.5(6.1, 6.6)
glutamate(Glu)	7.8(7.4, 9.0)	9.0(8.5, 9.8)	8.2(8.0, 9.0)
Glu+Gln(Glx)	11.3(9.9, 13.2)	13.3(10.5, 14.0)	12.8(9.0, 15.7)
total choline(Cho)	2.3(2.1, 2.4)	2.2(2.1, 2.3)	2.2(2.2, 2.4)
MM09	7.2(6.2, 7.6)	6.4(5.6, 7.1)	6.8(6.4, 7.5)
MM20	13.5(11.7, 14.2)	10.3(9.5, 13.0)	11.8(10.6, 14.8)
T1 Signal Intensity Index	1.8(1.6, 1.9)	2.1(1.9, 2.1)**,#	1.8(1.8, 1.9)
T2* (ms)	55.4(51.0, 60.6)	49.0(42.5, 54.9)	54.8(49.9, 56.3)

Globus Pallidus			
	Controls	Welders	Smelters
T1 Signal Intensity Index	2.7(2.5, 2.9)	3.8(3.5, 4.1)**	3.2(3.0, 3.3)*

* p<0.05,

** p<0.01, for comparison between each Mn-exposed group and controls;

p<0.05, for comparison between welders and smelters.